water

MDPI

Article

Preparation of CeO_2 Supported on Graphite Catalyst and Its Catalytic Performance for Diethyl Phthalate Degradation during Ozonation

Xin-Yi Tao, Yu-Hong Cui * and Zheng-Qian Liu

School of Environmental Science and Engineering, Huazhong University of Science and Technology, Wuhan 430074, China; txy523616717@163.com (X.-Y.T.); zhengqianliu@hust.edu.cn or zhengqianliu@126.com (Z.-Q.L.)

* Correspondence: yhcui@hust.edu.cn

Abstract: Catalysts for the efficient catalytic decomposition of ozone to generate reactive free radicals to oxidize pollutants are needed. The graphite-supported CeO_2 catalyst was optimally prepared, and its activity in ozonation was evaluated using the degradation of diethyl phthalate (DEP) as an index. The stability of CeO_2/graphite catalyst and the influence of operating conditions on its catalytic activity were investigated, and the mechanism of CeO_2/graphite catalytic ozonation was analyzed. CeO_2/graphite had the highest catalytic activity at a Ce load of 3.5% and a pyrolysis temperature of 400 °C with the DEP degradation efficiency of 75.0% and the total organic carbon (TOC) removal efficiency of 48.3%. No dissolution of active components was found during the repeated use of CeO_2/graphite catalyst. The ozone dosage, catalyst dosage, initial pH, and reaction temperature have positive effects on the DEP degradation by CeO_2/graphite catalytic ozonation. The presence of *tert*-butanol significantly inhibits the degradation of DEP at an initial pH of 3.0, 5.8, or 9.0, and the experimental results of the •OH probe compound *p*CBA indicate that the CeO_2/graphite catalyst can efficiently convert ozone into •OH in solution. The DEP degradation in the CeO_2/graphite catalytic ozonation mainly depends on the •OH in the bulk solution formed by ozone decomposition.

Keywords: graphite; ozonation; diethyl phthalate; cerium oxide; catalyst

Citation: Tao, X.-Y.; Cui, Y.-H.; Liu, Z.-Q. Preparation of CeO_2 Supported on Graphite Catalyst and Its Catalytic Performance for Diethyl Phthalate Degradation during Ozonation. *Water* **2024**, *16*, 1274. https://doi.org/10.3390/w16091274

Academic Editor: Alexandre T. Paulino

Received: 16 March 2024
Revised: 16 April 2024
Accepted: 25 April 2024
Published: 29 April 2024

1. Introduction

Heterogeneous catalytic processes are receiving increasing attention in water treatment due to their advantages of low secondary pollution and recyclability [1]. Various catalysts with different carriers and different active components have been prepared, studied, and applied in organic pollutants removal in various catalytic processes, including Fenton-like processes [2], persulfate processes [3], catalytic ozonation [4], photocatalysis [5,6], electrocatalysis [7,8], and various combined processes, etc. Appropriate carriers and active components loaded on them are particularly important for catalyst performance and its stability [1]. Carbon materials have received extensive attention as catalysts or catalyst carriers for ozonation in the past two decades [9,10]. As one of the carbon materials, the specific surface area of graphite is relatively small, and its S_{BET} usually does not exceed 20 m^2/g [11–13]. Correspondingly, the total amount of active sites that graphite can provide is relatively small [13,14], and the catalytic activity of graphite is usually not high if it is used as a catalyst directly during ozonation [11–13]. Therefore, some researchers have pretreated graphite (e.g., ball milling) to increase its specific surface area [13,15], or have directly used high surface area graphite [14], expanded graphite [16–18], graphite felt [19], graphene, and its oxides [19] with a larger specific surface area as catalysts or catalyst carriers to improve its catalytic activity.

Our group has always preferred to directly use graphite as the catalyst carrier, and Pt was used as the active component in the earliest studies, although the catalytic activity

and stability are excellent [20]. Considering the high cost of Pt, we subsequently used ZnO as the active component loaded on graphite, and the catalyst shows high catalytic activity for DEP degradation, while its stability is not good [12]. The catalyst prepared by loading CeO_2 on activated carbon exhibits good catalytic activity and stability in ozonation [21,22]. Therefore, this study attempted to load CeO_2 on graphite to investigate its catalytic activity and stability in ozonation.

In the present study, a CeO_2 supported on graphite (CeO_2/graphite) catalyst was optimally prepared, and its catalytic activity and stability were investigated. Diethyl phthalate (DEP) is used as an indicator to characterize the activity of CeO_2/graphite catalyst because it is difficult to be oxidized by ozone (k = 0.14 M^{-1} s^{-1}) [23] and is easily oxidized by $^{\bullet}OH$ (k = 3.98 × 10^9 M^{-1} s^{-1}) [24]. The influence of reaction parameters on the catalytic activity of CeO_2/graphite was investigated, and the reaction mechanism of DEP degradation by CeO_2/graphite catalytic ozonation was discussed according to the results of $^{\bullet}OH$ quenching experiments and the evaluation experiments on its ability to decompose ozone to produce $^{\bullet}OH$.

2. Experimental

2.1. Materials and Reagents

Commercial powdered graphite (1 μm ≥ 60%) was obtained from the Hendeli Graphite Factory (Qingdao, China). All chemicals used for experiments were analytical grade reagents, and ultrapure water was used for all experiments.

2.2. Preparation of Catalysts

$Ce(NO_3)_2$ was used as the metal precursor, and the CeO_2/graphite catalyst was produced by the equal volume impregnation method. The catalyst was dried in an oven at 105 °C for overnight after impregnation. Subsequently, it was pyrolyzed at a certain temperature for 3 h in an N_2 atmosphere. Without special statement, the loading amount of Ce and the pyrolysis temperature were 3.5 wt.% and 400 °C, respectively.

2.3. Characterization of Catalysts

The XRD patterns of CeO_2/graphite catalysts were recorded on a D/max-rB XRD instrument (Rigaku, Akishima, Japan), using Cu Kα radiation (λ = 0.15406 nm) and equipped with graphite monochromator, with an operating voltage of 45 kV and current of 50 mA. The surface morphology of the CeO_2/graphite catalyst was characterized using a field-emission SEM (Quanta 200F, Hillsboro, OR, USA) and a TEM (Hitachi H-800, Maharashtra, India). A mass titration method was adopted to measure the point of zero charge (PZC) of graphite and CeO_2/graphite catalysts [25,26].

2.4. Ozonation Alone and Catalytic Ozonation Procedure

The experiments of ozonation alone and catalytic ozonation were carried out in a semi-batch mode. Ozone was produced from pure oxygen in a DHX-I ozone generator (Harbin Jiujiu Electric Chemical Engineering Ltd., Harbin, China), then ozone was continuously bubbled through a porous porcelain pellet into 1.0 L of aqueous solution containing DEP. In the experiments of catalytic ozonation, ozone was introduced into the reactor immediately after the catalyst being dosed into the solution, which corresponds to the start of the reaction. The reaction temperature was controlled at 20 ± 1 °C. Without special statement, the initial DEP concentration was 3 μM, the ozone flow rate was 0.38 mg min^{-1} when oxygen flow rate was controlled at 50 mL min^{-1}, and the initial pH of the DEP solution was 5.8 without any adjustment. The concentrated $HClO_4$ and NaOH solutions were adopted to adjust the initial pH of the reaction solution to investigate the influence of the initial pH on the performance of the CeO_2/graphite catalyst.

Urs von Gunten defined the ratio of $^{\bullet}OH$ exposure to ozone exposure as R_{ct}, which is used to express the conversion of ozone into $^{\bullet}OH$ in a given system [27,28]. To determine the R_{ct} values of ozone alone and catalytic ozonation in the present study, the initial pH

of the reaction solution was adjusted to 7.1 using the concentrated $HClO_4$ and NaOH solutions, and a small stock solution of scavenger (*tert*-butanol, TBA) and •OH probe compound (*p*-chlorobenzoic acid, *p*CBA) was added to the aqueous solution (1 L) to reach concentrations of 1 μM and 80 μM, respectively. The ozonation experiment was started by dosing a 50 mg/L catalyst and a small amount of ozone stock solution to the reactor to achieve an initial ozone concentration of 2 mg/L. At a given reaction time, the sample was withdrawn from the reactor and added directly to the indigo solution to quench the residual ozone [29].

2.5. Analytical Methods

The concentrations of DEP and *p*CBA were analyzed by an HPLC-UV with a waters symmetry C18 column (5 μm × 4.6 mm × 150 mm), and the methanol/water was used as the mobile phase with a flow rate of 1 mL min^{-1}. The TOC was measured with a TOC Analyzer (Analytik jena Multi N/C 3100, Jena, Germany). The concentrations of ozone in gas phase and in aqueous solution were measured by the iodometric method [30] and the indigo method [29], respectively. The concentration of H_2O_2 that formed during the reaction was determined using a photometric method [31].

After each cycle of the reaction, the CeO_2/graphite catalyst was recovered by filtration, then washed with ultrapure water and dried at 105 °C for 24 h. The Ce concentration in the filtrate was determined by ICP (Perkin-Elmer optima 5300DV, Markham, ON, Canada).

3. Results and Discussion

3.1. Catalytic Activity Comparison of CeO_2/Graphite Catalyst with Other Catalyst

The DEP degradation efficiency was 12.4%, 50.2%, and 56.7% for graphite adsorption, ozonation alone and graphite catalytic ozonation, respectively (Figure 1a), and the TOC removal efficiency increased from 4.1% for ozonation alone to 14.5% for ozonation with graphite (Figure 1b). Zhang et al. have observed that graphite has the ability to promote ozone decomposition to generate hydroxyl radical (•OH) at the solid–liquid interface [32], which may be beneficial to the TOC removal.

As for the graphite supported metal oxide catalysts, the loading of ZnO or CeO_2 significantly improved the catalytic activity of graphite (Figure 1). The ZnO/graphite catalyst showed better performance than the CeO_2/graphite catalyst on DEP degradation as the degradation efficiency was 93.8% and 75.0% for ZnO/graphite and CeO_2/Graphite, respectively (Figure 1a). However, the TOC removal was quite different as the CeO_2/graphite catalyst showed better performance (48.3%) than the ZnO/graphite catalyst (35.5%) (Figure 1b). The results indicate that the CeO_2/graphite catalyst exhibited a better performance than the ZnO/graphite catalyst on the oxidation of transformation products formed during the DEP degradation process.

The concentration of metal ions in the solution after ozonation with graphite supported metal oxide catalysts were detected. After 10 min reaction, the concentration of zinc ions in the solution reached 0.54 mg/L, which means that the stability of the ZnO/graphite catalyst is not very good. However, no dissolution of the active components of the CeO_2/graphite catalyst was detected (Figure 1b). These results indicate that although the CeO_2/graphite catalyst is inferior to the ZnO/graphite catalyst in terms of DEP degradation, it is significantly better than the ZnO/graphite catalyst in terms of TOC removal and catalyst stability (Figure 1).

In order to investigate the stability of the CeO_2/graphite catalyst, repeated use of the catalyst on DEP ozonation was conducted, and the results are shown in Figure 2. During the four reuses, there was only a slight decrease on the performance of the CeO_2/graphite catalyst for DEP degradation and TOC removal. The concentration of metal ions in the solution was detected after CeO_2/graphite catalytic ozonation, and no dissolution of cerium ion was found (Figure 1b). This result indicates that the CeO_2/graphite catalyst has good stability, which may be the reason why its performance only changes slightly in the degradation of DEP and TOC removal during repeated use.

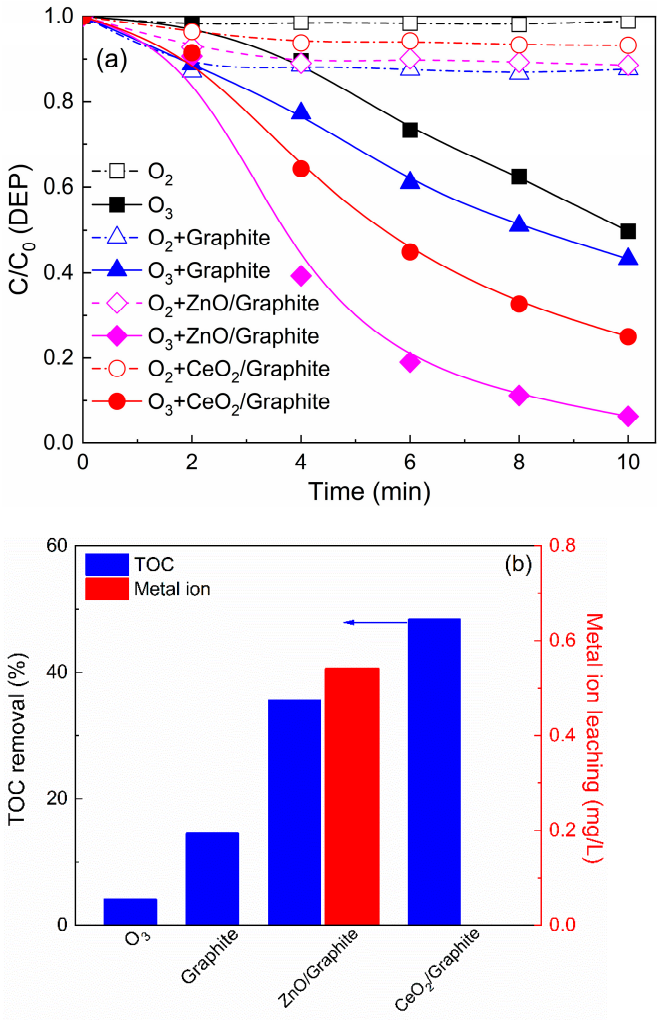

Figure 1. Comparison of DEP degradation during ozonation with graphite, ZnO/graphite, and CeO_2/graphite catalysts. (**a**) DEP concentration variation, (**b**) TOC removal, and metal ion leaching after 10 min reaction. Reaction conditions: T = 20 °C, initial pH = 5.8, initial DEP concentration = 3 μM, ozone gas concentration = 0.38 mg min^{-1}, catalyst dosage = 100 mg L^{-1}.

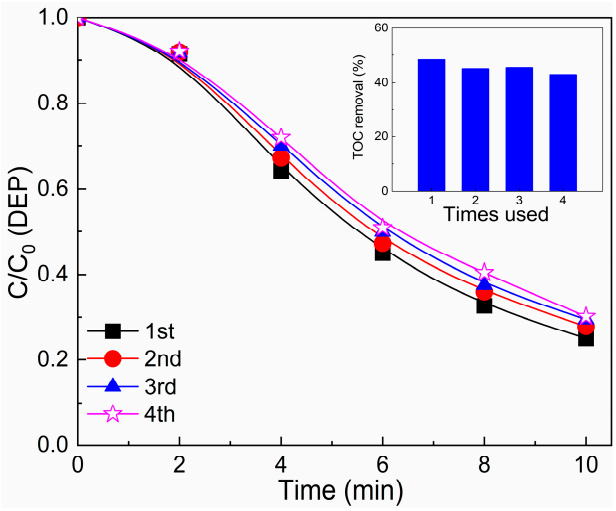

Figure 2. Reuse of the CeO_2/graphite catalyst during ozonation for the DEP degradation and TOC removal. Reaction conditions: T = 20 °C, initial pH = 5.8, initial DEP concentration = 3 μM, ozone gas concentration = 0.38 mg min^{-1}, catalyst dosage = 100 mg L^{-1}.

3.2. Optimization of CeO_2/Graphite Catalyst

The CeO_2/graphite catalyst with different amounts of cerium loading (1.0%, 2.0%, 3.5%, and 5.0%) was prepared to investigate its effect on the performance for DEP degradation during ozonation. As shown in Figure 3a, the DEP degradation efficiency increases with the cerium loading amount from 1.0% to 3.5% and decreases with the cerium loading amount from 3.5% to 5.0%. It is generally believed that the loading of metal oxides on the surface of carbon materials mainly depends on the oxygenated surface groups at the edges of plane and π electron structures at the inert basal plane of carbon materials [33–35]. The surface groups, such as carboxyl, hydroxyl, and carbonyl groups, are beneficial for nucleation of metal ions, which are reduced to nanoscale particles. As for the inert basal plane, the surface π electron structures act as Lewis basic sites and would lead to electron donor–acceptor complexes, which are strong interactions between metal particles and the carbon materials. Due to the fewer defects in graphite, the loading sites of metal oxides on the graphite surface may be mainly dependent on its π electron structures [36,37]. As for the present CeO_2/graphite catalysts, the binding sites on the graphite surface are progressively occupied with the increase in cerium loading amount from 1.0% to 3.5%. Hence, the available binding sites would be not enough with a further increase in cerium loading amount to 5.0%, and the agglomeration of CeO_2 nanoparticles may occur due to the limited binding sites on the graphite surface, leading to the decrease in catalytic activity just like other carbon supported metal oxides [12,33,38].

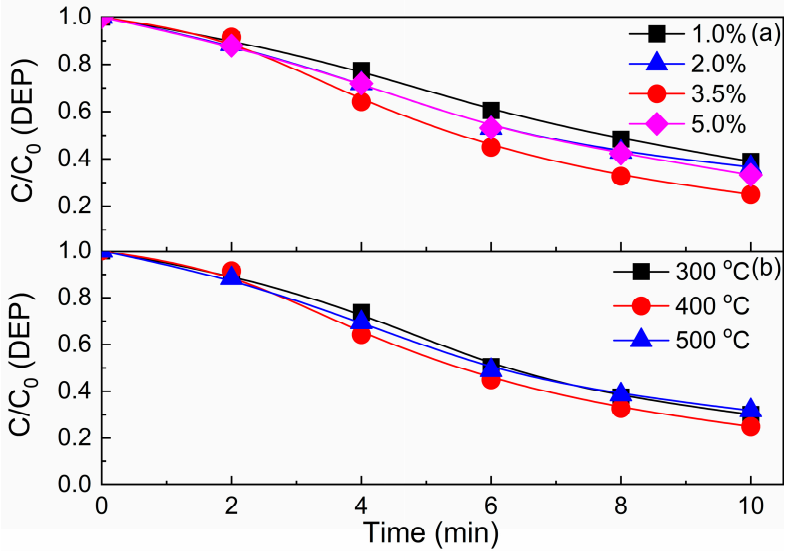

Figure 3. Effect of (**a**) cerium loading amount and (**b**) pyrolysis temperature on ozonation of DEP with CeO_2/graphite catalysts. Reaction conditions for ozonation: T = 20 °C, initial pH = 5.8, initial DEP concentration = 3 μM, ozone gas concentration = 0.38 mg min^{-1}, catalyst dosage = 100 mg L^{-1}. Reaction conditions for catalyst preparation: T = 400 °C for (**a**), cerium loading amount = 3.5% for (**b**).

The pyrolysis temperature usually has a significant impact on the activity of the prepared catalyst. A series of CeO_2/graphite catalysts were prepared to investigate the effect of pyrolysis temperature (300 °C, 400 °C, and 500 °C) on DEP degradation during catalytic ozonation. As shown in Figure 3b, the DEP degradation efficiency increases with the pyrolysis temperature from 300 °C to 400 °C and decreases slightly with the pyrolysis temperature from 400 °C to 500 °C.

3.3. Characterization of CeO_2/Graphite Catalyst

The prepared CeO_2/graphite catalysts were characterized by SEM, TEM, and XRD. The cerium loading and pyrolysis did not have significant impacts on the surface morphology of the graphite (Figure 4a), except that a lot of small particles with good dispersion are attached to the surface of graphite (Figure 4b) which should be cerium oxide formed

by pyrolysis of the active component Ce impregnated on graphite. XRD patterns of CeO_2/graphite catalysts prepared under different conditions are shown in Figure 4c,d. For comparison, the XRD result of graphite (0% cerium loading amount) is also presented. The CeO_2/graphite catalysts prepared under various conditions exhibited CeO_2 characteristic diffraction peaks at 2θ of 28.44°, 33.16°, 47.34°, and 56.46° [39,40], which demonstrates that the active component of the prepared CeO_2/graphite catalyst is in the form of CeO_2.

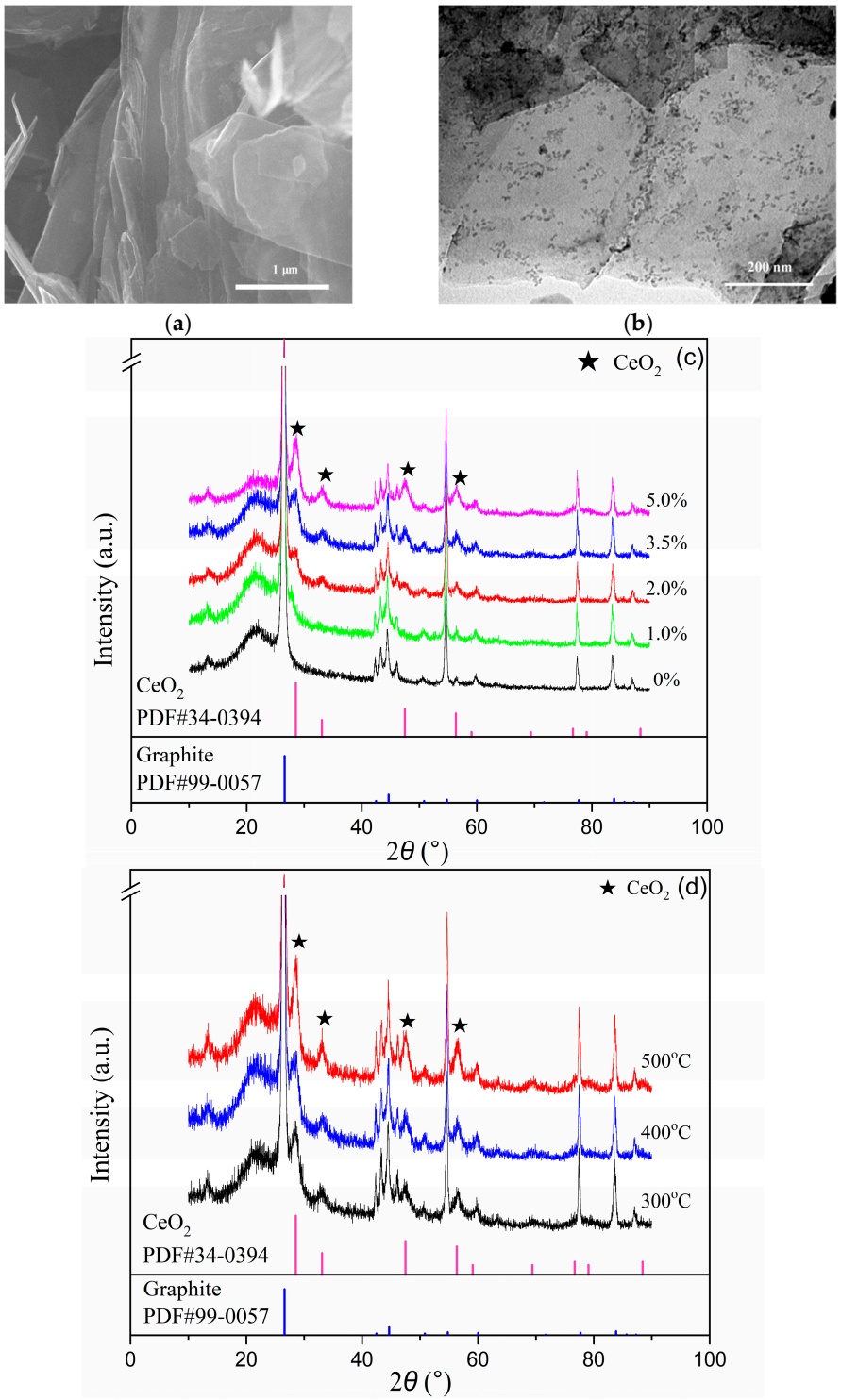

Figure 4. Characterization of CeO_2/graphite catalysts. (**a**) SEM (×80,000), (**b**) TEM (×100,000), XRD patterns with different (**c**) cerium loading amount and (**d**) pyrolysis temperature. Reaction conditions for catalyst preparation: T = 400 °C for (**a**–**c**), cerium loading amount = 3.5% for (**a**,**b**,**d**).

As shown in Figure 4c, the intensity of diffraction peaks for CeO_2 gradually increases with the increase in cerium loading amount, indicating that the CeO_2 grains generated on the graphite surface gradually increase. Since the active component of the CeO_2/graphite catalyst is in the form of CeO_2, the increase in CeO_2 grains on the graphite surface is helpful for the increase in active sites. At this point, an appropriate increase in cerium loading amount (from 0% to 3.5%) can increase the active sites on the catalyst surface, thereby enhancing its catalytic activity for ozonation of DEP (Figure 3a). However, the sites on the graphite surface that can bind the active component is limited. When the cerium loading amount further increases (from 3.5% to 5.0%), CeO_2 can only deposit on the original sites due to the lack of binding sites on the graphite surface. The agglomeration of CeO_2 grains may lead to a decrease in the active component dispersion on the graphite surface, which in turn leads to a decrease in the activity of the Ce/graphite catalyst (Figure 3a).

Figure 4d shows the effect of pyrolysis temperature on XRD patterns of the CeO_2/graphite catalyst. The intensity of diffraction peaks for CeO_2 gradually increases with the increase in pyrolysis temperature. On the one hand, increasing the pyrolysis temperature is beneficial for the crystallization of the active component, forming structurally intact CeO_2 grains, which is conducive to the catalytic activity improvement of the CeO_2/graphite catalyst (Figure 3b). On the other hand, increasing the pyrolysis temperature makes CeO_2 grains more prone to agglomeration, leading a decrease in the active sites, which in turn leads to a decrease in the activity of the CeO_2/graphite catalyst (Figure 3b).

3.4. Effect of Operation Conditions on the Performance of CeO_2/Graphite Catalyst

3.4.1. Effect of Ozone Dosage and Catalyst Dosage

The influence of ozone dosage on the DEP degradation was investigated during ozonation with CeO_2/graphite, and the results of ozonation alone are also presented for comparison (Figure 5). Ozone dosage had a remarkable influence on the DEP degradation during both ozonation alone and CeO_2/graphite catalytic ozonation, as the DEP degradation efficiency increased from 42.6% to 76.9% during ozonation alone and from 59.2% to 84.6% during CeO_2/graphite catalytic ozonation with ozone dosage increasing from 0.14 mg/min to 0.68 mg/min, respectively. It should be pointed that although increasing ozone dosage can improve the primary DEP transformation efficiency, ozonation alone may not be able to convert other organic substances, such as organic intermediates during the DEP degradation, which is clearly different from CeO_2/graphite catalytic ozonation as the latter shows good performance on TOC removal (Figure 1b).

The influence of catalyst dosage on the DEP degradation were investigated during ozonation with CeO_2/graphite, and the results of ozonation with graphite are also shown for comparison (Figure 6). Catalyst dosage only had a slight influence on the DEP degradation during graphite catalytic ozonation, but had an apparent influence on the DEP degradation during CeO_2/graphite catalytic ozonation, as the DEP degradation efficiency increased from 55.7% to 60.6% during graphite catalytic ozonation and from 68.1% to 88.5% during CeO_2/graphite catalytic ozonation with catalyst dosage increasing from 50 mg/L to 200 mg/L, respectively. Compared to graphite catalytic ozonation, the improvement on DEP degradation efficiency was 12.4%, 17.9%, and 27.9% with CeO_2/graphite catalyst dosage of 50 mg/L, 100 mg/L, and 200 mg/L, respectively (Figure 6). Since the ozone dosage is enough for the reaction, the more CeO_2/graphite catalyst is dosed, the more active sites that can play catalytic roles. In this case, the reaction of ozone conversion into strong oxidizing free radicals is enhanced, thus improving the oxidation efficiency of the target organic compound.

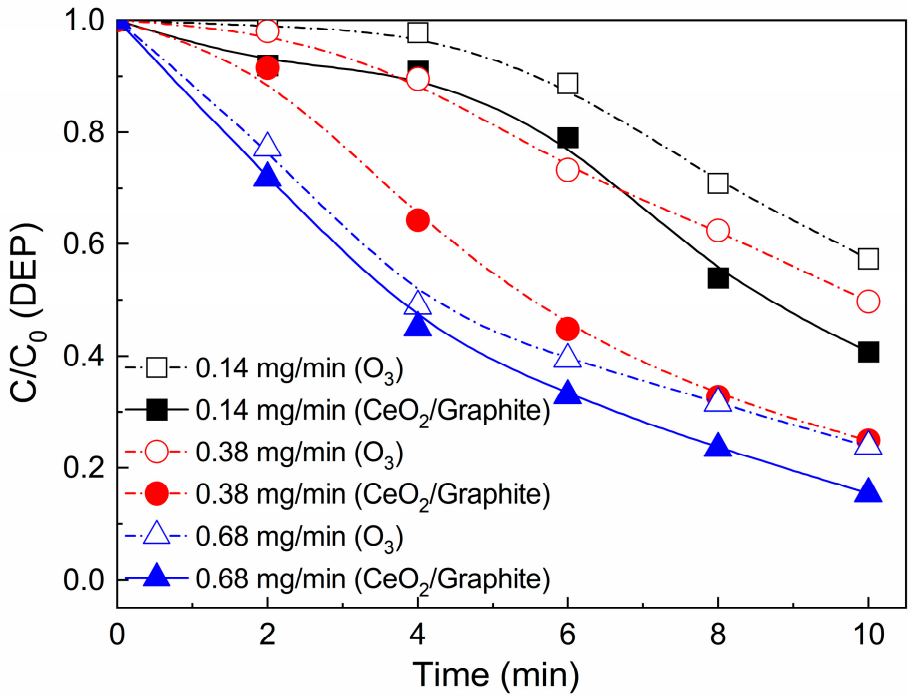

Figure 5. Effect of ozone dosage on DEP degradation during CeO_2/graphite catalytic ozonation. Reaction conditions: T = 20 °C, initial pH = 5.8, initial DEP concentration = 3 μM, catalyst dosage = 100 mg L^{-1}.

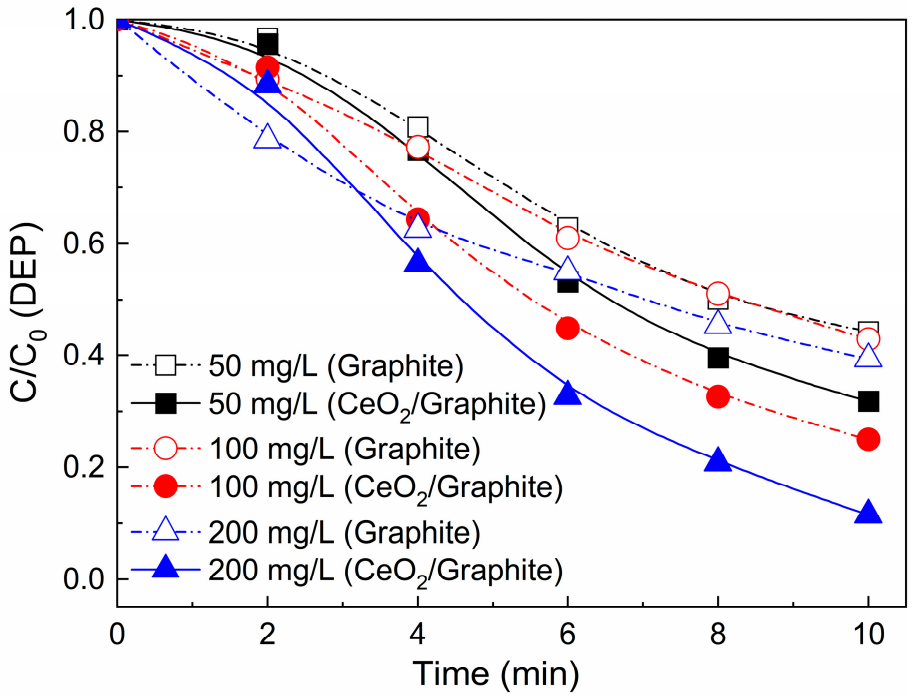

Figure 6. Effect of catalyst dosage on DEP degradation during CeO_2/graphite catalytic ozonation. Reaction conditions: T = 20 °C, initial pH = 5.8, initial DEP concentration = 3 μM, ozone gas concentration = 0.38 mg min^{-1}.

3.4.2. Effect of Initial DEP Concentration and Initial pH

The influence of initial DEP concentration on the DEP degradation were investigated during CeO_2/graphite catalytic ozonation, and the results are shown in Figure 7. The DEP degradation efficiency increased from 68.6% to 75.0% with an initial DEP concentration increasing from 1 μM to 3 μM. However, further increasing the initial DEP concentration

from 3 μM to 10 μM can lead to a decrease in the DEP degradation efficiency. For ozonation alone, the DEP degradation efficiency increased with initial DEP concentration increasing from 1 μM to 5 μM and decreased with initial DEP concentration increasing from 5 μM to 10 μM (inserted figure of Figure 7).

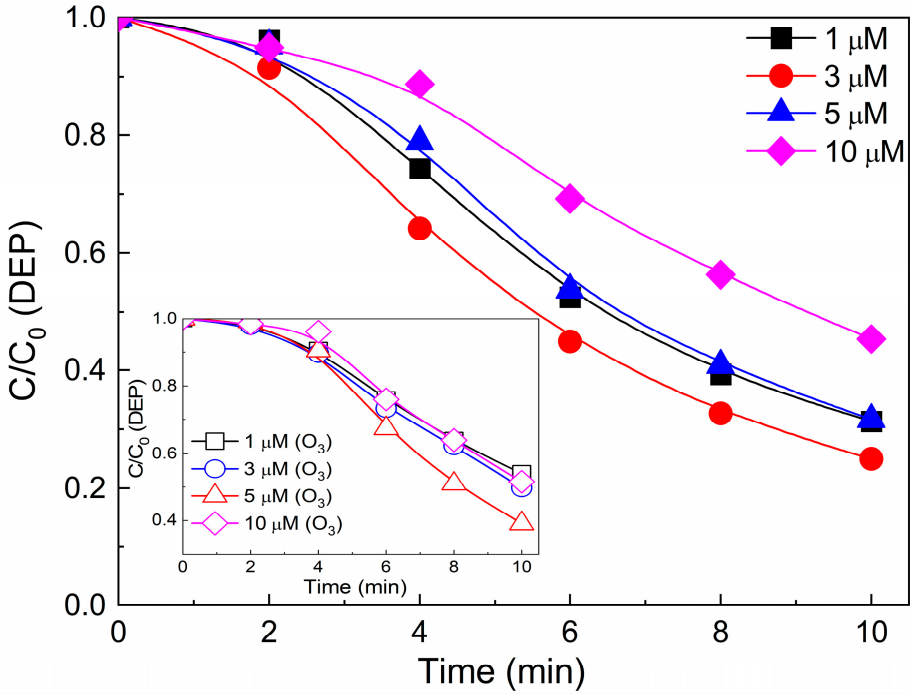

Figure 7. Effect of initial DEP concentration on DEP degradation during CeO_2/graphite catalytic ozonation. Reaction conditions: T = 20 °C, initial pH = 5.8, ozone gas concentration = 0.38 mg min^{-1}, catalyst dosage = 100 mg L^{-1}.

The influence of initial pH on the DEP degradation was investigated during CeO_2/graphite catalytic ozonation, and the results of ozonation alone are also presented for comparison (Figure 8). DEP degradation efficiency by ozonation alone significantly increased with the increase in the initial pH. It has been reported that ozone can hardly self-decomposed to generate •OH in aqueous solution at an initial pH of 3.0 [41]. Thus, the DEP degradation efficiency is low since it mainly relies on the slowly direct oxidation by ozone (k = 0.14 M^{-1} s^{-1}) [23]. Increasing the pH value of aqueous solution can increase the ozone decomposition rate to generate more •OH and can maintain a stable concentration of •OH in the aqueous solution [27], which may lead to a remarkable increase in the DEP degradation efficiency due to the fast reaction between DEP and •OH ($k = 3.98 \times 10^9$ M^{-1} s^{-1}) [24].

With the presence of the CeO_2/graphite catalyst, ozone decomposition was accelerated and generated •OH in aqueous solution even at an initial pH of 3.0, thus DEP degradation efficiency increased from 7.9% of ozonation alone to 56.9% of CeO_2/graphite catalytic ozonation (Figure 8). The metal ion in the solution after ozonation with CeO_2/graphite catalyst at the initial pH 3.0 was determined to be 0.18 mg/L. To investigate the possible influence of the leaching metal ion on DEP degradation during ozonation, the experiment was carried out and the results are presented in the inserted figure of Figure 8. The DEP degradation efficiency was 38.5% during ozonation with 0.18 mg/L Ce^{4+}, which is much higher than that of ozonation alone (7.9%) but lower than that of CeO_2/graphite catalytic ozonation (56.9%). This result indicates that the metal ion (Ce^{4+}) leaching from CeO_2/graphite catalyst does have a certain catalytic effect in ozonation, but the CeO_2 supported on the graphite surface also plays a catalytic role in the DEP degradation.

At an initial pH of 5.8, the DEP degradation efficiency during CeO_2/graphite catalytic ozonation was 75.0%, which is significantly higher than that of ozonation alone (50.2%)

(Figure 8). However, at an initial pH of 9.0, the improvement effect on DEP degradation efficiency by CeO_2/graphite catalyst addition is not as remarkable as in the acidic or neutral solution. A reasonable explanation is that ozone self-decomposes more quickly at an initial pH of 9.0 [27], and the effect of CeO_2/graphite catalyst in promoting ozone decomposition at this pH is not as significant as that at lower pH. Though ozonation alone in alkaline solution can achieve similar effects as CeO_2/graphite catalytic ozonation, for the convenience of subsequent treatment and to save reagents, most water treatment is recommended to be carried out under neutral or near neutral conditions, and CeO_2/graphite catalytic ozonation have advantages over ozonation alone from this point of view.

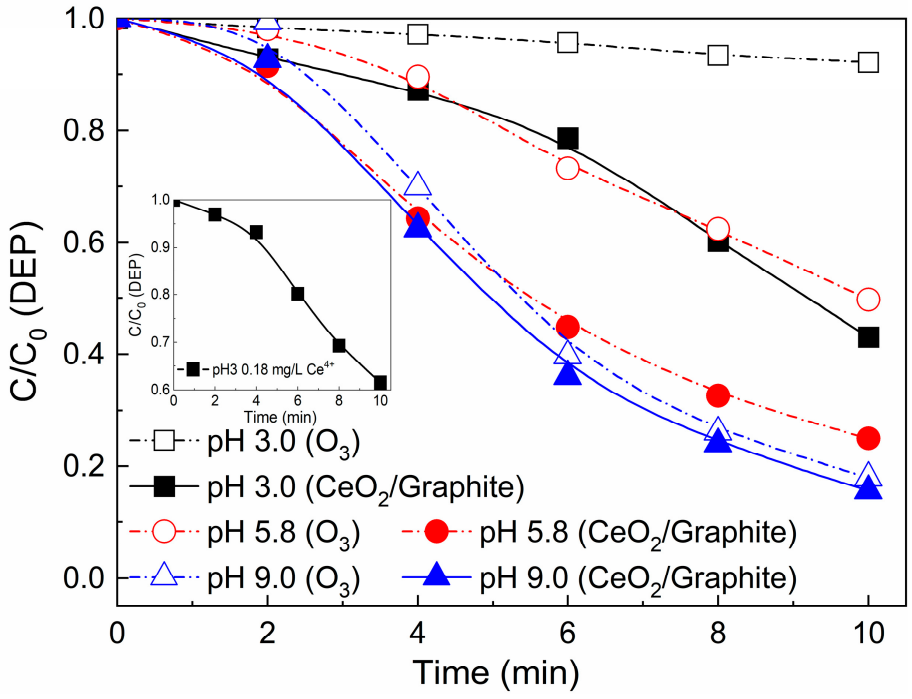

Figure 8. Effect of initial pH on DEP degradation during CeO_2/graphite catalytic ozonation. Reaction conditions: T = 20 °C, initial DEP concentration = 3 μM, ozone gas concentration = 0.38 mg min^{-1}, catalyst dosage = 100 mg L^{-1}.

3.4.3. Effect of Reaction Temperature

The influence of reaction temperature, ranging from 10 °C to 40 °C on the DEP degradation, was investigated during CeO_2/graphite catalytic ozonation, and the results during ozonation alone are also presented for comparison (Figure 9). Within the temperature range of this study, raising the reaction temperature is beneficial for DEP degradation both in ozonation alone and in CeO_2/graphite catalytic ozonation, especially in the range of 10 °C to 30 °C. Though DEP degradation efficiency during CeO_2/graphite catalytic ozonation is always better than that during ozonation alone, the gap between these two processes significantly reduces at high reaction temperature (above 20 °C). A reasonable explanation is that the increase in water temperature can not only promote the decomposition of ozone to produce more •OH [27], but also accelerate the reaction between the generated •OH and DEP [24], which makes the catalytic effect in promoting ozone decomposition and DEP degradation not as remarkable as that at low temperature. However, most water treatment is carried out at room temperature (around 20 °C) since raising the water temperature requires a significant energy consumption. Thus, CeO_2/graphite catalytic ozonation has advantages over ozonation alone from this point of view.

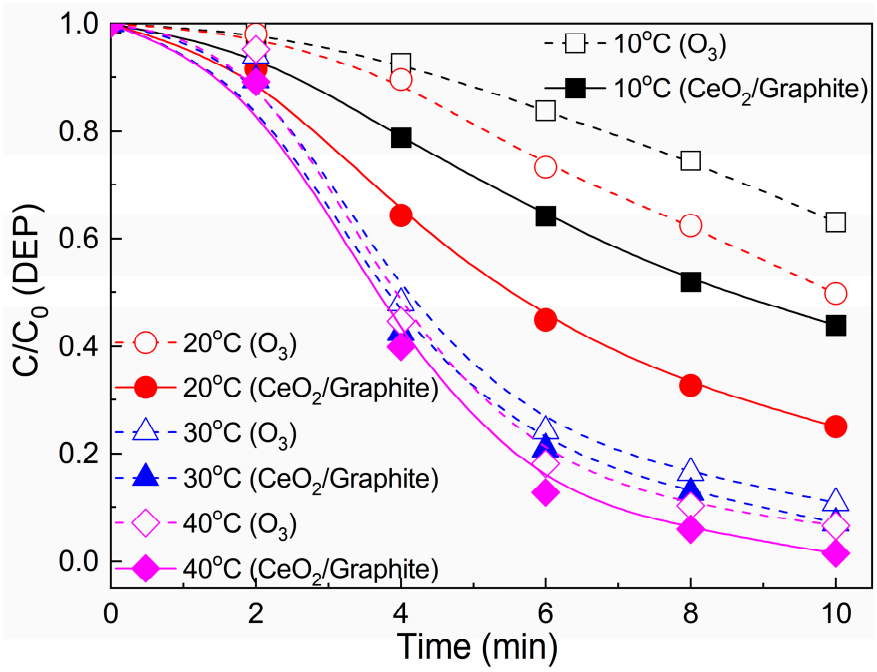

Figure 9. Effect of reaction temperature on DEP degradation during CeO_2/graphite catalytic ozonation. Reaction conditions: initial pH = 5.8, initial DEP concentration = 3 μM, ozone gas concentration = 0.38 mg min^{-1}, catalyst dosage = 100 mg L^{-1}.

3.5. Reaction Mechanism of CeO_2/Graphite Catalytic Ozonation

3.5.1. Evolution of Ozone Concentration and Hydrogen Peroxide Concentration

The variations of both aqueous ozone concentration and gaseous ozone concentration were investigated for ozonation alone, graphite catalytic ozonation, and CeO_2/graphite catalytic ozonation (Figure 10). It was found that the difference in gaseous ozone concentration was almost negligible among the three processes during the whole reaction. However, the aqueous ozone concentration in the three processes showed significant differences as the reaction prolonged and the order of dissolved ozone concentration was ozonation alone > CeO_2/graphite catalytic ozonation > graphite catalytic ozonation (Figure 10). The consumption of ozone during the ozonation process comes from the self-decomposition of ozone, the catalytic ozone decomposition, and the DEP oxidation. For the ozonation alone process, only the self-decomposition of ozone and the DEP oxidation would consume ozone, resulting in the highest residual ozone concentration in the aqueous solution (Figure 10). For graphite and CeO_2/graphite catalytic ozonation processes, in addition to the self-decomposition of ozone and the DEP oxidation, the presence of catalysts also catalyzes the decomposition of ozone to generate free radicals (such as •OH) to promote the DEP degradation, thus their residual ozone concentrations in the aqueous solution are lower than that of the ozonation alone process (Figure 10). It is interesting that the residual aqueous ozone concentration in the CeO_2/graphite catalytic ozonation process is higher than that of graphite though the DEP degradation efficiency by CeO_2/graphite catalytic ozonation is higher than that of graphite catalytic ozonation. It is well-known that different catalysts have different catalytic efficiencies on decomposition of ozone into •OH [42], hence, a possible reason for the above results is that the CeO_2/graphite catalyst can more effectively transfer ozone into •OH than the graphite catalyst, resulting in better DEP degradation efficiency with less ozone consumption (Figures 1 and 10).

The variation of H_2O_2 concentrations during ozonation alone, graphite catalytic ozonation, and CeO_2/graphite catalytic ozonation was investigated (Figure 11). It has been reported that the reducing sites on the surface of carbon materials (such as π electron structures and basic oxygenated groups) can reduce dissolved oxygen to produce a certain amount of H_2O_2 in aqueous solution [38,43,44]. In this study, the generation of H_2O_2

during the CeO_2/graphite adsorption process was also investigated by replacing O_3 with O_2 (Figure 11). The loading of CeO_2 had little effect on the evolution of H_2O_2 concentration on graphite during adsorption process but had a significant effect on the evolution of H_2O_2 concentration in catalytic ozonation, and the order of H_2O_2 concentration is ozonation alone > graphite catalytic ozonation > CeO_2/graphite catalytic ozonation (Figure 11). It has been reported that the intermediate product H_2O_2 reacts with the ozone adsorbed on the surface of AC to generate •OH [45], resulting in a lower H_2O_2 concentration in AC catalytic ozonation compared to ozonation alone [45–47]. This is consistent with the lower concentration of H_2O_2 during catalytic ozonation with graphite or CeO_2/graphite compared to ozonation alone in this study. Additionally, CeO_2 also has a strong ability to decompose H_2O_2 [48], which may be the reason for the lowest H_2O_2 concentration in the CeO_2/graphite catalytic ozonation among the three oxidation processes.

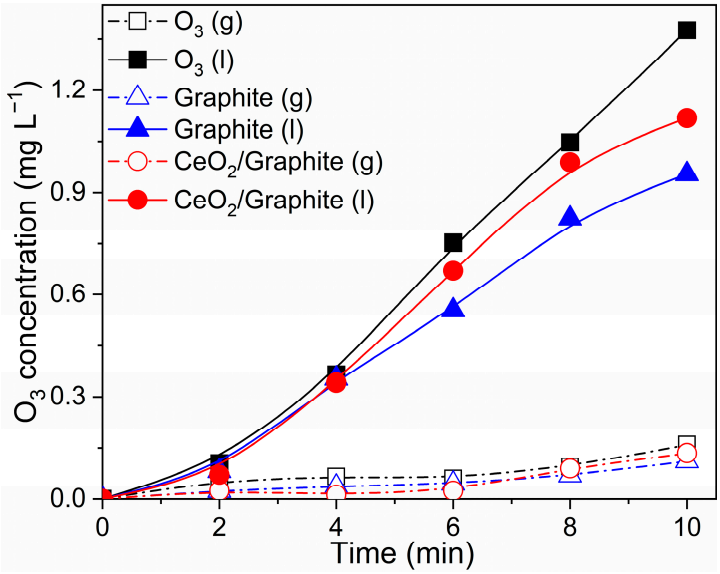

Figure 10. Evolution of ozone concentration during CeO_2/graphite catalytic ozonation. Reaction conditions: T = 20 °C, initial pH = 5.8, initial DEP concentration = 3 μM, ozone gas concentration = 0.38 mg min^{-1}, catalyst dosage = 100 mg L^{-1}.

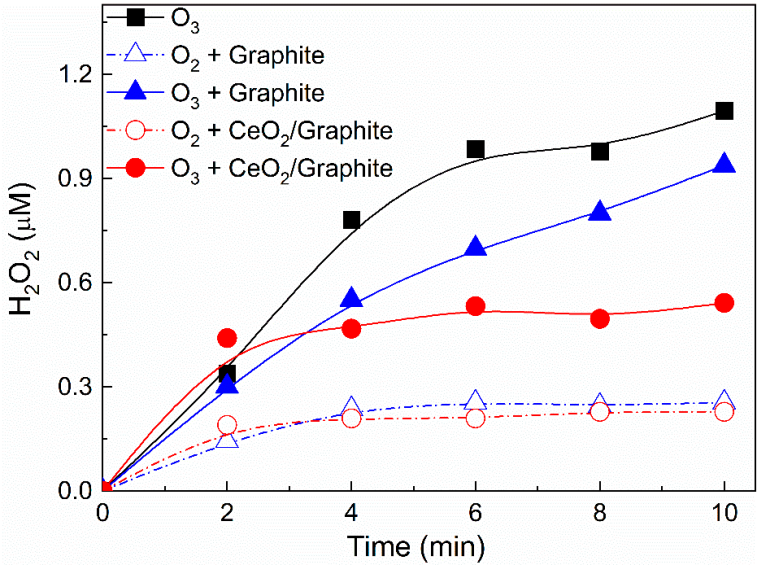

Figure 11. Evolution of H_2O_2 concentration during CeO_2/graphite catalytic ozonation. Reaction conditions: T = 20 °C, initial pH = 5.8, initial DEP concentration = 3 μM, ozone gas concentration = 0.38 mg min^{-1}, catalyst dosage = 100 mg L^{-1}.

3.5.2. Effect of the Presence of TBA

It is generally believed that the DEP degradation in ozone-based advanced oxidation processes follows the •OH reaction mechanism [49–53]. Thus, the role of •OH in the present study was investigated using TBA as a radical scavenger, as TBA reacts very quickly with •OH ($k = 6 \times 10^8$ M^{-1} s^{-1}) [27] and very slowly with ozone ($k = 0.001$ M^{-1} s^{-1}) [23,52]. The effect of TBA addition on ozonation of DEP with or without the CeO_2/graphite catalyst is shown in Figure 12.

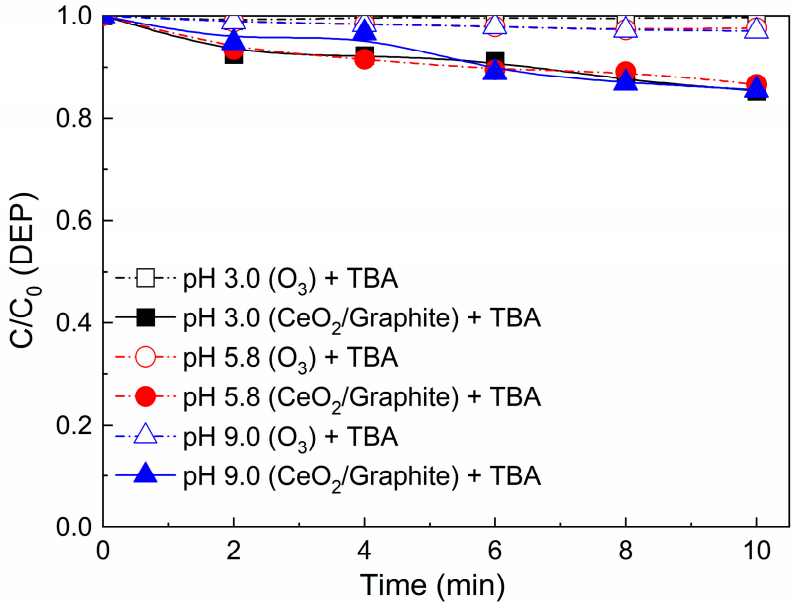

Figure 12. Effect of TBA on ozonation of DEP with or without CeO_2/graphite catalyst under different initial pH. Reaction conditions: T = 20 °C, initial DEP concentration = 3 μM, ozone gas concentration = 0.38 mg min^{-1}, catalyst dosage = 100 mg L^{-1}.

The DEP degradation was almost completely inhibited with TBA addition during ozonation alone at pH 3.0, 5.8, and 9.0 (Figure 12) which should be because the •OH derived from ozone decomposition has been completely quenched by TBA and the reaction rate between DEP and ozone is very slow as aforementioned. The DEP degradation significantly decreased with TBA addition during CeO_2/graphite catalytic ozonation at pH 3.0, 5.8, and 9.0, as the DEP degradation efficiency did not exceed 15% at all the three initial pH values (Figure 12) while it was 56.9%, 75.0%, and 84.3% at pH 3.0, 5.8, and 9.0 without TBA addition, respectively (Figure 8). These results demonstrate that •OH plays an important role in DEP degradation during CeO_2/graphite catalytic ozonation.

3.5.3. Discussion of the Reaction Mechanism

As mentioned above, the quenching experiments of TBA show that •OH plays a key role in the DEP degradation during CeO_2/graphite catalytic ozonation. Urs von Gunten proposed the concept of R_{ct} (Equation (1)) [28] and thought that it could be used to characterize the ability of catalysts on ozone decomposition to generate •OH [53,54], as shown in Equation (1).

$$R_{ct} = \frac{\int [\bullet OH]dt}{\int [O_3]dt} = \frac{\ln [pCBA]_t / [pCBA]_0}{-k_{\bullet OH,pCBA}} \times \frac{1}{\int [O_3]dt} \quad (1)$$

The terms of $\int [O_3]dt$ and $\int [\bullet OH]dt$ represent the time-integrated concentration of ozone and •OH, which is equal to ozone exposure and •OH exposure, respectively. The R_{ct} values for ozone alone and ozonation with different catalysts can be obtained using Equation (1) to process the data in Figure 13. As shown in Table 1, the R_{ct} value for ozone

alone was 1.13×10^{-9}, which is similar to the R_{ct} value of 1.0×10^{-9} previously reported in the literature [55]. The R_{ct} value for ozonation with graphite and graphite supported metal oxides catalysts in this study is similar to that of graphene oxide [56] and some granular activated carbon [53,55], but smaller than that of carbon nanotubes [55] and graphene oxide supported metal oxides [56]. Interestingly, although the graphite catalyst is not as effective as the CeO_2/graphite catalyst in the degradation of DEP and *p*CBA (Figures 1 and 13a), it had a larger R_{ct} value (Table 1). Although the •OH exposure of the graphite catalytic ozonation is smaller than that of CeO_2/graphite (Figure 13a), it decomposes more ozone than CeO_2/graphite (Figure 13b) and makes its ozone exposure smaller (Table 1). Thus, the graphite catalyst has a larger R_{ct} value in ozonation since R_{ct} is the ratio of •OH exposure to ozone exposure. Overall, the graphite catalyst has greater R_{ct} value than the CeO_2/graphite catalyst, mainly because it improves ozone utilization efficiency rather than •OH yield [57].

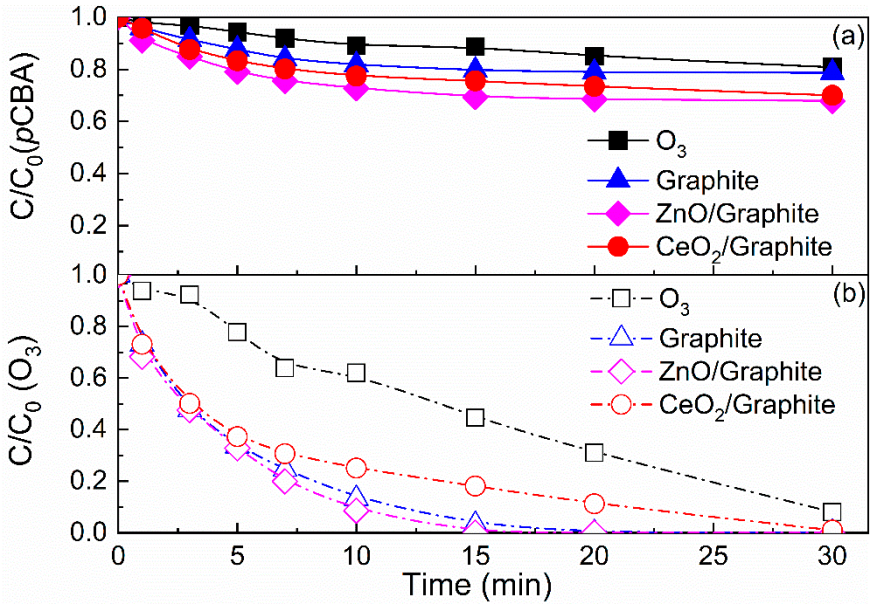

Figure 13. *p*CBA degradation and ozone decomposition in ozonation alone and ozonation with different catalysts. Reaction conditions: T = 20 °C, initial pH = 7.1, initial *p*CBA concentration = 1 μM, initial TBA concentration = 80 μM, initial ozone concentration = 2 mg L^{-1}, catalyst dosage = 50 mg L^{-1}.

Table 1. R_{ct} and $R_{OH,O3}$ values of ozonation alone and ozonation with different catalysts.

Process	O_3 Exposure (M•s)	•OH Exposure (M•s)	R_{ct}	$R_{OH,O3}$ (s)
O_3	3.78×10^{-2}	4.26×10^{-11}	1.13×10^{-9}	9.84×10^{-7}
O_3 + Graphite	9.38×10^{-3}	4.75×10^{-11}	5.21×10^{-9}	1.63×10^{-6}
O_3 + ZnO/Graphite	9.21×10^{-3}	7.30×10^{-11}	7.26×10^{-9}	1.94×10^{-6}
O_3 + CeO_2/Graphite	1.60×10^{-2}	7.13×10^{-11}	4.10×10^{-9}	2.29×10^{-6}

In order to better characterize the ability of catalysts to decompose ozone to generate •OH, we introduced the concept of R_{OH,O_3} proposed by Kwon et al., which is the ratio of •OH exposure to the amount of ozone consumption (Equation (2)) [58].

$$R_{OH,O_3} = \frac{R_{ct}}{k_{O_3}} = \frac{\int [\bullet OH]dt}{\int [O_3]dt \times k_{O_3}} = \frac{\int [\bullet OH]dt}{[O_3]_0 \times (1 - e^{k_{O_3} \bullet t})} = \frac{\int [\bullet OH]dt}{[O_3]_0 - [O_3]_t} = \frac{\int [\bullet OH]dt}{\Delta [O_3]_t} \quad (2)$$

The term of $\Delta[O_3]_t$ represents the total ozone consumption at time t of the reaction. Similarly, the R_{OH,O_3} values for ozonation alone and ozonation with different catalysts can be obtained by processing the data in Figure 13 with Equation (2). As can be seen from Table 1, the R_{OH,O_3} value increased in the order of O_3+CeO_2/graphite > O_3+ZnO/

graphite > O_3+graphite > O_3. An interesting thing is that although the CeO_2/graphite catalyst is not as effective at degrading DEP and *p*CBA as the ZnO/graphite catalyst (Figures 1 and 13a), it has greater R_{OH,O_3} value (Table 1). This means that the CeO_2/graphite catalyst is more efficient at converting dissolved ozone into •OH than the ZnO/graphite catalyst.

Different researchers have different views on the reaction mechanism of ozonation with carbon materials [10]. Some believe that the degradation reaction of organic compounds follows the surface reaction mechanism, some believe that it follows the bulk solution reaction mechanism, and some researchers believe that it follows the combined effect of the surface reaction and the bulk solution reaction [32,59–61]. In the present study, if surface reactions play a role in the DEP degradation, when the initial pH of the solution changes from 3.0 to 9.0, it will cause a change on the surface charged state of CeO_2/graphite catalyst from positive to negative as the pH_{PZC} of this catalyst is 7.2 [62], which will inevitably affect the adsorption and decomposition of ozone on its surface due to the electrophilic property of ozone [27]. Subsequently, the contribution of surface reactions will change, and the degradation efficiency of DEP will also be affected.

Previous studies have shown that TBA has little adsorption on the surface of carbon materials [60], so it can completely inhibit the DEP degradation through the bulk solution reaction, but it is difficult to inhibit the DEP degradation through surface reactions [32]. However, the degradation efficiency of DEP is almost the same at different initial pH (3.0, 5.8, or 9.0) in the presence of TBA during ozonation with CeO_2/graphite (Figure 8). Therefore, it can be inferred that the contribution of surface reaction to DEP degradation is almost negligible, and the DEP degradation mainly depends on the •OH generated by the bulk solution reaction during CeO_2/graphite catalytic ozonation. Actually, the above discussion of R_{ct} and R_{OH,O_3} has proven that the CeO_2/graphite catalyst has a good ability to convert ozone into •OH in bulk solution (Table 1). In general, CeO_2/graphite is a good catalyst, both in terms of its effectiveness in DEP degradation and TOC removal, and from the perspective of catalyst stability.

4. Conclusions

The CeO_2/graphite catalyst can not only decompose DEP effectively during ozonation, but also remove TOC effectively, and the active component CeO_2 loaded on graphite shows good stability during repeated use. The optimal preparation conditions for CeO_2/graphite catalyst were a Ce loading of 3.5% and a pyrolysis temperature of 400 °C.

The degradation efficiency of DEP increases as the ozone dosage increases within the range of 0.14 mg/min to 0.68 mg/min for both ozonation alone and CeO_2/graphite catalytic ozonation. Catalyst dosage (50–200 mg/L) has a remarkable influence on the DEP degradation during CeO_2/graphite catalytic ozonation. The degradation efficiency of DEP first increases and then decreases with the increase in its initial concentration (1–10 μM) for CeO_2/graphite catalytic ozonation. The increase in both initial pH (3.0–9.0) and reaction temperature (10–40 °C) can promote the degradation of DEP for CeO_2/graphite catalytic ozonation.

The DEP degradation is significantly inhibited with the addition of TBA during CeO_2/graphite catalytic ozonation for initial pH 3.0, 5.8, or 9.0, and the results of R_{ct} and R_{OH,O_3} indicate that the CeO_2/graphite catalyst has a good ability to convert ozone into •OH in bulk solution. The DEP degradation should mainly depend on the •OH generation in the bulk solution during CeO_2/graphite catalytic ozonation.

Author Contributions: X.-Y.T.: Investigation, writing—original draft preparation; Y.-H.C.: Conceptualization, methodology, supervision, writing—review and editing; Z.-Q.L.: Funding acquisition, investigation, data curation. All authors have read and agreed to the published version of the manuscript.

Funding: This research was funded by the National Key R&D Program of China, grant number 2022YFE0105600.

Data Availability Statement: Data will be made available on request.

Conflicts of Interest: The authors declare no conflicts of interest.

References

1. Parvulescu, V.I.; Epron, F.; Garcia, H.; Granger, P. Recent Progress and Prospects in Catalytic Water Treatment. *Chem. Rev.* **2022**, *122*, 2981–3121. [CrossRef] [PubMed]
2. Li, L.; Liu, S.; Cheng, M.; Lai, C.; Zeng, G.; Qin, L.; Liu, X.; Li, B.; Zhang, W.; Yi, Y.; et al. Improving the Fenton-like catalytic performance of MnO_x-Fe_3O_4/biochar using reducing agents: A comparative study. *J. Hazard. Mater.* **2021**, *406*, 124333. [CrossRef] [PubMed]
3. Yan, Y.; Wei, Z.; Duan, X.; Long, M.; Spinney, R.; Dionysiou, D.D.; Xiao, R.; Alvarez, P.J.J. Merits and limitations of radical vs. nonradical pathways in persulfate-based advanced oxidation processes. *Environ. Sci. Technol.* **2023**, *57*, 12153–12179. [CrossRef]
4. Liu, Z.-Q.; Han, B.-J.; Wen, G.; Ma, J.; Wang, S.-J.; Zha, R.-G.; Shen, L.-P.; Wang, C. Full-scale application of catalytic ozonation for drinking water treatment: Case study in China. *J. Environ. Eng.* **2014**, *140*, A5013002. [CrossRef]
5. Ghiyasiyan-Arani, M.; Masjedi-Arani, M.; Salavati-Niasari, M. Size controllable synthesis of cobalt vanadate nanostructures with enhanced photocatalytic activity for the degradation of organic dyes. *J. Mol. Catal. A Chem.* **2016**, *425*, 31–42. [CrossRef]
6. Mazloom, F.; Masjedi-Arani, M.; Ghiyasiyan-Arani, M.; Salavati-Niasari, M. Novel sodium dodecyl sulfate-assisted synthesis of $Zn_3V_2O_8$ nanostructures via a simple route. *J. Mol. Liq.* **2016**, *214*, 46–53. [CrossRef]
7. Cui, Y.H.; Li, X.Y.; Chen, G. Electrochemical degradation of bisphenol A on different anodes. *Water Res.* **2009**, *43*, 1968–1976. [CrossRef] [PubMed]
8. Hu, R.; Yang, S.Q.; Li, J.Y.; Sun, F.; Liu, Z.Q.; Yang, J.; Cui, Y.H.; Zhang, B. Insight into micropollutant abatement during ultraviolet light-emitting diode combined electrochemical process: Reaction mechanism, contributions of reactive species and degradation routes. *Sci. Total Environ.* **2023**, *876*, 162798. [CrossRef] [PubMed]
9. Yang, J.; Fu, L.; Wu, F.; Chen, X.; Wu, C.; Wang, Q. Recent developments in activated carbon catalysts based on pore size regulation in the application of catalytic ozonation. *Catalysts* **2022**, *12*, 1085. [CrossRef]
10. Liu, Z.Q.; Li, J.Y.; Li, S.T. Catalytic Ozonation over Activated Carbon-based Materials. In *Advanced Ozonation Processes for Water and Wastewater Treatment: Active Catalysts and Combined Technologies*; Cao, H., Xie, Y., Wang, Y., Xiao, J., Eds.; Royal Society of Chemistry: Croydon, UK, 2022; pp. 85–122.
11. Oh, S.-Y.; Nguyen, T.-H.A. Ozonation of phenol in the presence of biochar and carbonaceous materials: The effect of surface functional groups and graphitic structure on the formation of reactive oxygen species. *J. Environ. Chem. Eng.* **2022**, *10*, 107386. [CrossRef]
12. Liu, Z.-Q.; Tu, J.; Wang, Q.; Cui, Y.-H.; Zhang, L.; Wu, X.; Zhang, B.; Ma, J. Catalytic ozonation of diethyl phthalate in aqueous solution using graphite supported zinc oxide. *Sep. Purif. Technol.* **2018**, *200*, 51–58. [CrossRef]
13. Jiménez-López, M.A.; Rey, A.; Rivas, F.J.; Beltrán, F.J. Water ozone decomposition in graphitic and graphene based catalytic materials: Kinetics of catalyst deactivation. *Catal. Today* **2024**, *430*, 114541. [CrossRef]
14. Bernat-Quesada, F.; Espinosa, J.C.; Barbera, V.; Álvaro, M.; Galimberti, M.; Navalón, S.; García, H. Catalytic ozonation using edge-hydroxylated graphite-based materials. *ACS Sustain. Chem. Eng.* **2019**, *7*, 17443–17452. [CrossRef]
15. Jiménez-López, M.A.; Rey, A.; Montes, V.; Beltrán, F.J. Testing carbon structures for metal-free catalytic/photocatalytic ozonation to remove disinfection by-product formation potential. *Sep. Purif. Technol.* **2024**, *329*, 125156. [CrossRef]
16. He, J.; Song, W.; Gao, Z.; Huang, X. Calcium carbonate/expanded graphite as an efficient catalyst for catalytic ozonation of ethylenediaminetetraacetic acid. *Environ. Eng. Sci.* **2020**, *37*, 450–456. [CrossRef]
17. Song, Y.; Feng, S.; Qin, W.; Ma, J. Mechanism of catalytic ozonation in expanded graphite aqueous suspension for the degradation of organic acids. *Environ. Technol.* **2023**, *44*, 739–750. [CrossRef]
18. He, J.; Song, W.; Huang, X.; Gao, Z. Preparation, characterization, and catalytic activity of a novel MgO/expanded graphite for ozonation of Cu-EDTA. *Environ. Sci. Pollut. Res.* **2021**, *28*, 39513–39523. [CrossRef]
19. Zhang, X.; Shen, T.; Ding, Y.; Tong, S. Graphite felt supported MgO catalytic ozonation of bisphenol A. *Ozone Sci. Eng.* **2019**, *41*, 541–550. [CrossRef]
20. Liu, Z.Q.; Ma, J.; Zhao, L. Preparation, Characterization and catalytic activity of Pt/graphite catalyst. *Chin. J. Inorg. Chem.* **2006**, *22*, 2263–2268. (In Chinese)
21. Liu, Z.Q.; Cui, Y.H.; Wang, M.Y.; Zheng, Y.J.; Zhong, Z.X.; Wu, X.H.; Wang, Z.; Zhang, B.P. Ozonation of oxytetracycline in the presence of activated carbon supported cerium oxide. *Environ. Eng. Manag. J.* **2016**, *15*, 2231–2237. [CrossRef]
22. Orge, C.A.; Órfão, J.J.M.; Pereira, M.F.R. Catalytic ozonation of organic pollutants in the presence of cerium oxide–carbon composites. *Appl. Catal. B Environ.* **2011**, *102*, 539–546. [CrossRef]
23. Yao, C.C.D.; Haag, W.R. Rate constants for direct reactions of ozone with several drinking water contaminants. *Water Res.* **1991**, *25*, 761–773. [CrossRef]
24. Wen, G.; Ma, J.; Liu, Z.-Q.; Zhao, L. Ozonation kinetics for the degradation of phthalate esters in water and the reduction of toxicity in the process of O_3/H_2O_2. *J. Hazard. Mater.* **2011**, *195*, 371–377. [CrossRef]
25. Noh, J.S.; Schwarz, J.A. Effect of HNO_3 treatment on the surface acidity of activated carbons. *Carbon* **1990**, *28*, 675–682. [CrossRef]
26. Liu, Z.-Q.; Ma, J.; Cui, Y.-H. Carbon nanotube supported platinum catalysts for the ozonation of oxalic acid in aqueous solutions. *Carbon* **2008**, *46*, 890–897. [CrossRef]

27. von Sonntag, C.; von Gunten, U. *Chemistry of Ozone in Water and Wastewater Treatment: From Basic Principles to Applications*; IWA Publishing: London, UK, 2012.
28. Elovitz, M.S.; von Gunten, U. Hydroxyl radical/ozone ratios during ozonation processes. I. The rct concept. *Ozone Sci. Eng.* **1999**, *21*, 239–260. [CrossRef]
29. Bader, H.; Hoigné, J. Determination of ozone in water by the indigo method. *Water Res.* **1981**, *15*, 449–456. [CrossRef]
30. Rakness, K.; Gordon, G.; Langlais, B.; Masschelein, W.; Matsumoto, N.; Richard, Y.; Robson, C.M.; Somiya, I. Guideline for measurement of ozone concentration in the process gas from an ozone generator. *Ozone Sci. Eng.* **1996**, *18*, 209–229. [CrossRef]
31. Bader, H.; Sturzenegger, V.; Hoigné, J. Photometric method for the determination of low concentrations of hydrogen peroxide by the peroxidase catalyzed oxidation of N,N-diethyl-p-phenylenediamine (DPD). *Water Res.* **1988**, *22*, 1109–1115. [CrossRef]
32. Zhang, S.; Quan, X.; Zheng, J.-F.; Wang, D. Probing the interphase "HO• zone" originated by carbon nanotube during catalytic ozonation. *Water Res.* **2017**, *122*, 86–95. [CrossRef] [PubMed]
33. Van Dam, H.E.; Van Bekkum, H. Preparation of platinum on activated carbon. *J. Catal.* **1991**, *131*, 335–349. [CrossRef]
34. Lu, J.; Do, I.; Drzal, L.T.; Worden, R.M.; Lee, I. Nanometal-decorated exfoliated graphite nanoplatelet based glucose biosensors with high sensitivity and fast response. *ACS Nano* **2008**, *2*, 1825–1832. [CrossRef]
35. Beltran, F.J.; Alvarez, P.M.; Gimeno, O. Graphene-Based catalysts for ozone processes to decontaminate water. *Molecules* **2019**, *24*, 3438. [CrossRef]
36. Ishii, T.; Kaburagi, Y.; Yoshida, A.; Hishiyama, Y.; Oka, H.; Setoyama, N.; Ozaki, J.-I.; Kyotani, T. Analyses of trace amounts of edge sites in natural graphite, synthetic graphite and high-temperature treated coke for the understanding of their carbon molecular structures. *Carbon* **2017**, *125*, 146–155. [CrossRef]
37. Coloma, F.; Sepulveda-Escribano, A.; Fierro, J.L.G. Rodriguez-Reinoso, Preparation of platinum supported on pregraphitized carbon blacks. *Langmuir* **1994**, *10*, 750–755. [CrossRef]
38. Leon, C.A.L.Y.; Solar, J.M.; Calemma, V.; Radovic, L.R. Evidence for the protonation of basal plane sites on carbon. *Carbon* **1992**, *30*, 797–811. [CrossRef]
39. Fijolek, L.; Wolski, L. Bifunctional $CePO_4/CeO_2$ nanocomposite as a promising heterogeneous catalyst for the enhancement of the ozonation recovery effect in the presence of chloride ions. *Sci. Rep.* **2022**, *12*, 9043. [CrossRef]
40. Zhang, J.; Dong, B.; Liu, J.; Yang, W.; Ge, S.; He, S. The role of Mn doping on Ce-based γ-Al_2O_3 catalysts for phenol degradation. *Environ. Eng. Sci.* **2021**, *39*, 56–63. [CrossRef]
41. Kasprzyk-Hordern, B.; Ziółek, M.; Nawrocki, J. Catalytic ozonation and methods of enhancing molecular ozone reactions in water treatment. *Appl. Catal. B Environ.* **2003**, *46*, 639–669. [CrossRef]
42. Zhang, S.; Quan, X.; Wang, D. Catalytic ozonation in arrayed zinc oxide nanotubes as highly efficient mini-column catalyst reactors (MCRs): Augmentation of hydroxyl radical exposure. *Environ. Sci. Technol.* **2018**, *52*, 8701–8711. [CrossRef] [PubMed]
43. Hossain, M.S.; Tryk, D.; Yeager, E. The electrochemistry of graphite and modified graphite surfaces: The reduction of O_2. *Electrochim. Acta* **1989**, *34*, 1733–1737. [CrossRef]
44. Ahumada, E.; Lizama, H.; Orellana, F.; Suárez, C.; Huidobro, A.; Sepúlveda-Escribano, A.; Rodrı, F. Catalytic oxidation of Fe(II) by activated carbon in the presence of oxygen: Effect of the surface oxidation degree on the catalytic activity. *Carbon* **2002**, *40*, 2827–2834. [CrossRef]
45. Beltran, F.J.; Pocostales, P.; Alvarez, P.; Oropesa, A.L. Diclofenac removal from water with ozone and activated carbon. *J. Hazard. Mater.* **2009**, *163*, 768–776. [CrossRef] [PubMed]
46. Beltrán, F.J.; García-Araya, J.F.; Giráldez, I. Gallic acid water ozonation using activated carbon. *Appl. Catal. B Environ.* **2006**, *63*, 249–259. [CrossRef]
47. Beltrán, F.J.; Giráldez, I.; García-Araya, J.F. Kinetics of activated carbon promoted ozonation of polyphenol mixtures in water. *Ind. Eng. Chem. Res.* **2008**, *47*, 1058–1065. [CrossRef]
48. Zhang, T.; Chen, W.; Ma, J.; Qiang, Z. Minimizing bromate formation with cerium dioxide during ozonation of bromide-containing water. *Water Res.* **2008**, *42*, 3651–3658. [CrossRef] [PubMed]
49. Mohan, S.; Mamane, H.; Avisar, D.; Gozlan, I.; Kaplan, A.; Dayalan, G. Treatment of diethyl phthalate leached from plastic products in municipal solid waste using an ozone-based advanced oxidation process. *Materials* **2019**, *12*, 4119. [CrossRef] [PubMed]
50. Mansouri, L.; Tizaoui, C.; Geissen, S.U.; Bousselmi, L. A comparative study on ozone, hydrogen peroxide and UV based advanced oxidation processes for efficient removal of diethyl phthalate in water. *J. Hazard. Mater.* **2019**, *363*, 401–411. [CrossRef] [PubMed]
51. Jabesa, A.; Ghosh, P. Removal of diethyl phthalate from water by ozone microbubbles in a pilot plant. *J. Environ. Manag.* **2016**, *180*, 476–484. [CrossRef]
52. Hoigné, J.; Bader, H. Rate constants of reactions of ozone with organic and inorganic compounds in water—I. *Water Res.* **1983**, *17*, 173–183. [CrossRef]
53. Sánchez-Polo, M.; von Gunten, U.; Rivera-Utrilla, J. Efficiency of activated carbon to transform ozone into OH radicals: Influence of operational parameters. *Water Res.* **2005**, *39*, 3189–3198. [CrossRef] [PubMed]
54. Sanchez-Polo, M.; Salhi, E.; Rivera-Utrilla, J.; von Gunten, U. Combination of ozone with activated carbon as an alternative to conventional advanced oxidation processes. *Ozone Sci. Eng.* **2006**, *28*, 237–245. [CrossRef]

55. Oulton, R.; Haase, J.P.; Kaalberg, S.; Redmond, C.T.; Nalbandian, M.J.; Cwiertny, D.M. Hydroxyl radical formation during ozonation of multiwalled carbon nanotubes: Performance optimization and demonstration of a reactive CNT filter. *Environ. Sci. Technol.* **2015**, *49*, 3687–3697. [CrossRef] [PubMed]
56. Jothinathan, L.; Hu, J. Kinetic evaluation of graphene oxide based heterogenous catalytic ozonation for the removal of ibuprofen. *Water Res.* **2018**, *134*, 63–73. [CrossRef] [PubMed]
57. Long, J.; Guo, Y.; Yu, G.; Komarneni, S.; Wang, Y. Evaluation of the effect of catalysts on ozone mass transfer and pollutant abatement during laboratory catalytic ozonation experiments: Implications for practical water and wastewater treatment. *ACS EST Eng.* **2022**, *3*, 387–397. [CrossRef]
58. Kwon, M.; Kye, H.; Jung, Y.; Yoon, Y.; Kang, J.-W. Performance characterization and kinetic modeling of ozonation using a new method: ROH,O_3 concept. *Water Res.* **2017**, *122*, 172–182. [CrossRef] [PubMed]
59. Liu, Y.; Chen, C.; Duan, X.; Wang, S.; Wang, Y. Carbocatalytic ozonation toward advanced water purification. *J. Mater. Chem. A* **2021**, *9*, 18994–19024. [CrossRef]
60. Beltran, F.J.; Rivas, F.J.; Fernandez, L.A.; Alvarez, P.M.; Montero-de-Espinosa, R. Kinetics of catalytic ozonation of oxalic acid in water with activated carbon. *Ind. Eng. Chem. Res.* **2002**, *41*, 6510–6517. [CrossRef]
61. Faria, P.C.C.; Órfão, J.J.M.; Pereira, M.F.R. Activated carbon catalytic ozonation of oxamic and oxalic acids. *Appl. Catal. B Environ.* **2008**, *79*, 237–243. [CrossRef]
62. Werner, S.; Morgan, J.J. *Aquatic chemistry: Chemical Equilibria and Rates in Natural Waters*, 3rd ed.; Wiley: New York, NY, USA, 1996.